UILU-ENG 84-3604

Report No. 104

MODELING OF HEAT FLOW IN BONDED SAND MOLDS

by

J. A. Dantzig and S. C. Lu*
Department of Mechanical and Industrial Engineering, UIUC
*Presently with Packard Electric Company, Warren, OH

A Report of the
MATERIALS ENGINEERING - MECHANICAL BEHAVIOR
College of Engineering, University of Illinois at Urbana-Champaign
February 1984

ABSTRACT

A method has been developed for the representation of the abstraction of heat from castings into bonded sand molds. The method consists of representing the local surface geometry by a plane, cylinder or sphere, based on the local heat flow environment. The characteristics of the heat flow into the mold for that surface shape are used to specify a set of boundary conditions on the casting.

The technique has been implemented in an existing finite element method program to compute heat flow in solidifying castings. An example is included, with results compared to experiments.

TABLE OF CONTENTS

INTRODUCTION

In recent years, much effort has been put into the improvement of productivity in manufacturing processes, particularly through the use of computer simulation. These methods are finding increasing application in the foundry casting industry, because they offer the possibility of reducing the costs of design and production of new parts. Heat transfer analysis of the cooling of castings is being used to evaluate various parts designs, and to aid in the placement of gates and risers.

By their nature, foundry castings are nearly always complex shapes. Accordingly, most simulations of castings solidification use the finite element method (FEM) because it is best suited to handling irregular geometries. A significant drawback of this method is that the cost of simulating the solidification of a given part can be very high. The manpower time to generate the FEM model, and the computer time required to solve the solidification problem are both substantial.

An attractive means for reducing both of these costs is to solve the solidification problem in the casting without explicitly solving the heat flow problem in the mold. Instead, only the casting is modeled, and the mold is represented by appropriate boundary conditions applied on the surface of the casting. This means is attractive because the solution in the mold material is usually of (relatively) less interest. Furthermore, the node density must be high in the mold region, due to its low conductivity compared to that of the metal being cast, so that the size of the problem can be greatly reduced by eliminating these nodes from the analysis. Finally, because the model is much smaller, it is much easier to generate.

Formulation of these boundary conditions has been discussed by Niyama [1], and by Wei, et. al., [2,3]. They have termed the replacement of nodes in

the mold by heat flux boundary conditions the Q-dot method. The essence of the method is to recognize that the heat fluxes in the casting and the mold must balance at the interface. Thus, if the temperature in the mold is known, the effect of the mold can be completely described by computing the heat flux at the interface. In the work to date, certain special shapes, for which analytical solutions can be found, have been used to supply the boundary conditions. The method has the following limitations, however: (1) only two-dimensional problems have been modeled, because suitable three-dimensional analytical solutions are not available, and (2) it is not suitable for arbitrary shapes, because there is no way to account for the possibility that two (or more) shapes will be sufficiently close that their heat flow fields will overlap, thus invalidating the solution.

In this paper, methods will be presented for representation of the heat flow in the mold surrounding three-dimensional castings, by boundary conditions applied at the surface of the casting. Application is described in relation to bonded sand molds. The method consists of assigning a local curvature to the surface, and using the heat flux from such a curved surface as the boundary condition. Heat flow from other parts of the casting is accounted for by adjusting the local curvatures to correspond with the extent of heat flow. Implementation of the method in ANSYS, a commercial finite element solver, is described.

METHODS

The method which has been developed to handle to heat flow in the sand mold consists of three parts:

(a) Representation of heat flow surfaces

(b) Solution of heat flow problems in bonded sand molds

(c) Implementation in ANSYS

The parts are described in sequence.

(a) Representation of heat flow surfaces

It is necessary to recognize that the local heat flow from the surface of a casting depends on the local shape of the surface. Consider the solidification of a two-dimensional L-shaped casting, as in Fig. 1. This model was simulated with nodes in both the casting and the mold [4]. Shown are computed isotherms at 549 seconds after pouring. In the mold at the inner corner of the L, the isotherms resemble those inside a cylinder; along the edges the isotherms resemble those near a plane, and at the external corners, the isotherms resemble those outside a cylinder. The figure suggests the possibility of representing the heat flow from the surface of the casting by assuming that the heat flows into, or out from, a relatively simple geometric figure, such as a cylinder or plane. It is also clear from the figure, that different representations must be used at different locations on the surface.

Another aspect of the problem can be seen by referring to Fig. 2, which shows computed isotherms in the same casting and mold, but at 2950 seconds after pouring. It still appears that a series of cylinders and planes could be used to model the heat flow near the surface, but now the radii of the cylinders at corresponding locations would have to be very different from

those used at 549 seconds. In order for a method based on representation by simple geometric figures to be successful, it is necessary to determine the appropriate shapes a priori.

The curvature of the isotherms near any point on the surface of the casting reflects the heat flow from the entire surface in a neighborhood about the point. The extent of the neighborhood about each point which influences the heat flow can be estimated as ℓ;

$$\ell = \sqrt{\alpha t} \tag{1}$$

where α is the thermal diffusivity of the mold material, and t is time.

Using Eq. (1), one can see how the curvature of the isotherms can change over time, as heat from greater distances along the casting comes into play at each point. Moreover, the curvature of the isotherms can be estimated by choosing a "domain of influence," given by Eq. (1), and fitting a curve to the surface based on the shape of the casting in that domain. A relatively simple way to do this in two-dimensional parts would be to select a point on the surface, then choose two other points also lying on the surface, but at a distance ℓ, (given by Eq. (1)), from the principal point. A segment of a circle may then be fitted to these three points, and the surface would be represented as a cylinder with radius equal to the radius of the fitted circle.

If the coordinates of the three points are (x_1, y_1), (x_2, y_2), and (x_3, y_3), then the center of the arc is located at (x, y) given by:

$$\begin{bmatrix} x \\ y \end{bmatrix} = \frac{1}{D} \begin{bmatrix} 2(y_3 - y_2)(x_2^2 - x_1^2 + y_2^2 - y_1^2) - 2(y_2 - y_1)(x_3^2 - x_2^2 + y_3^2 - y_2^2) \\ -2(x_3 - x_2)(x_2^2 + y_2^2 - x_1^2 - y_1) + 2(x_2 - x_1)(x_3^2 + y_3^2 - x_2^2 - y_2^2) \end{bmatrix} \tag{2}$$

where

$$D = 4(x_2 - x_1)(y_3 - y_2) - 4(x_3 - x_2)(y_2 - y_1) \tag{3}$$

Clearly, the radius of the cylinder is

$$R = ((x_1 - x)^2 + (y_1 - y)^2)^{1/2} \tag{4}$$

As an example, this method has been applied to the L-shaped casting of Figs. 1 and 2, at several different times. The results are shown in Figs. 3 and 4. The fitted curves at several locations are shown in comparison to computed isotherms for the same time. The curvatures of the isotherms and the local curvatures calculated by Eqs. (1) through (4) are quite similar. This indicates that the heat flow characteristics are accurately represented by the computed curved surface.

The most effective way to apply this method is to assign a local curvature to the surface for each surface element. The heat flow from the surface would then be equal to that which would flow into a sand mold having matching curvature, as in the Q-dot method. The advantage to this method is that different values for the curvature may be used to describe the surface. The curvatures may all be adjusted over the course of a simulation to account for the increasing domain of influence of heat flow. The required number of changes for accurate solutions must be determined by (numerical) experiments.

A further generalization of this method for three-dimensional objects is to permit the surface to be represented by a sphere, as well as by a cylinder or a plane. The analogy between heat flow from a sphere and the heat flow near a three-dimensional corner is an example.

In dealing with surfaces in space, there are two curvatures to be determined, and the values of these may be used to select between surface types (plane, cylinder or sphere), as well as the proper radius. The neighboring points on the surface of the casting can be chosen in an analogous way to the method described for selecting the points in the case of two-dimensional parts. For the three-dimensional case, however, more points are necessary to obtain a complete representation of the surface. It should be noted that, although there are but three allowable surfaces for representation, the fact that the radius is allowed to vary parametrically makes it possible to obtain reasonable approximations to many different shapes.

A particular advantage of this method is that the heat flow problems to be solved for the sand mold are now all one-dimensional. Therefore, it is relatively easy to determine and characterize the solutions. To implement the boundary curvature method, a library of solutions to the heat flow problem in the sand mold from various (one-dimensional) shapes is required. The next section describes the methods used to obtain these solutions.

(b) Solution of one-dimensional heat flow problems in bonded sand molds

Before considering the general problem of heat flow in the various geometries, it is instructive to consider the following problem. Let the bonded sand mold initially be at temperature T_s, equal to the vaporization temperature of the binder. Assume that the mold is in ideal contact with a

plane wall held at temperature T_w. In this case, the temperature distribution in the mold is governed by the following set of equations:

$$\rho C_p \frac{\partial T}{\partial t} = \frac{\partial}{\partial x}\left(\kappa \frac{\partial T}{\partial x}\right) \qquad 0 \leq x \leq \delta(t) \qquad (5)$$

$$T = T_w \qquad x = 0 \qquad (6)$$

$$T = T_s \qquad x = \delta(t) \qquad (7)$$

$$\kappa \frac{\partial T}{\partial x} = \rho L_v \frac{d\delta}{dt} \qquad x = \delta(t) \qquad (8)$$

$$\delta = 0 \qquad t = 0 \qquad (9)$$

$$I = I_s \qquad t = 0 \qquad (10)$$

Where κ is the thermal conductivity, ρ the density, C_p the specific heat of the mold, L_v the heat of vaporization of the binder, and $\delta(t)$ the location of the dry sand-wet sand interface. If all of the properties are constant, the solution to Eqs. (5) through (10) is [5,6]:

$$T = T_s + \frac{T_w - T_s}{\text{erf } \gamma} \text{erf } \left(\frac{x}{\sqrt{4\alpha t}}\right) \qquad (11)$$

$$\delta = 2\gamma\sqrt{\alpha t} \qquad (12)$$

and γ is the root of

$$\gamma e^{\gamma^2} \text{erf } \gamma = \frac{C_p(T_w - T_s)}{L_v \sqrt{\pi}} \qquad (13)$$

and $\alpha = \frac{\kappa}{\rho C_p}$

The wall must supply heat to maintain the temperature at T_w. The amount of heat required is equal to the heat flux in the mold at x = 0, i.e.

$$q = \kappa \frac{\partial T}{\partial x} (x = 0) = \frac{T_w - T_s}{\text{erf } \gamma} \cdot \frac{\kappa}{\sqrt{\pi \alpha t}} \tag{14}$$

As far as the plane casting is concerned, everything which occurs in the mold is fully described by Eq. (14). This fact allows the use of solutions like Eq. (14) as boundary conditions on the surface of castings.

Two important features of Eq. (14) are that the heat flux is proportional to the temperature difference $(T_w - T_s)$; and that the heat flux decreases as $1/t^{1/2}$. When the more general cases are considered (below), these general characteristics are retained. The singularity in q at t = 0 is an artifact which disappears when the fixed temperature boundary condition at x = 0 is replaced by a convective heat transfer condition.

Consider the following one-dimensional transient heat conduction problem:

$$\rho C_p(T) \frac{\partial T}{\partial t} = \left(\frac{\partial}{\partial r} + \frac{a}{r}\right) \left(\kappa(T) \frac{\partial T}{\partial r}\right) \tag{15}$$

$$-\frac{1}{n} \kappa(T) \frac{\partial T}{\partial r} = h(T) (T - T_w) \qquad \text{at } r = R_o \tag{16}$$

$$\frac{1}{n} \kappa(T) \frac{\partial T}{\partial r} = \rho L_v \frac{d\delta}{dt} \qquad \text{on } r = R_o + n\delta \tag{17}$$

$$T = T_s \qquad \text{on } r = R_o + n\delta \tag{18}$$

$$T = T_s \qquad \text{at } t = 0 \qquad (19)$$

$$\delta = 0 \qquad \text{at } t = 0 \qquad (20)$$

where

T is the mold temperature,

ρ is the density of the mold material

$C_p(T)$ is the temperature dependent specific heat

$\kappa(T)$ is the temperature dependent thermal conductivity

$h(T)$ is the temperature dependent heat transfer coefficient

L_v is the latent heat of vaporization of the mold binder material

δ is the position of the dry sand/wet sand interface

r is the radial distance

R_o is the radius of the fixed boundary (0 for a plane)

t is the time

a is { $n \times 1$ for a cylinder; $n \times 2$ for a sphere; 0 for a plane

n is { $+1$ for diverging heat flow; -1 for converging heat flow.

This problem describes the general case of heat flow from a casting at fixed temperature into a bonded sand mold, when the casting is a segment of a sphere, cylinder or a plane. This problem is the generalization of Eqs. (5) through (10) for the geometric shapes which are the allowed representations for the surfaces of castings.

The difference between the solution to the problem posed in Eqs. (15) through (20), and the solution to the most general case in castings is that,

in general, the surface temperature of a casting varies with time, say $\phi(t)$. The solution to the heat flow problem with variable surface temperature can be computed from the solution to Eqs. (15) through (20) by use of Duhamel's Theorem. Referring to the solution to the problem with variable surface temperature as $\theta(r,t)$, the solutions are related as [6]:

$$\theta(r,t) = T_s + (T_w - T_s) \int_0^t (\phi(\lambda) - T_s) \frac{\partial}{\partial t} \left(\frac{T(r,t-\lambda) - T_s}{T_w - T_s}\right) d\lambda \quad (21)$$

However, if the surface temperature $\phi(t)$ changes very slowly in comparison with changes in the sand temperature, then Eq. (21) may be approximated as:

$$\theta(r,t) = T_s + (\phi(t) - T_s)\,(T(r,t) - T_s) \quad (22)$$

This may be shown by integrating Eq. (21) by parts. Thus, the solutions to Eqs. (15) through (20) contain sufficient information to characterize the most general case, represented by $\theta(r,t)$. The next task is to generate a catalog of solutions to Eqs. (15) through (20) for various values of R_o and n. These solutions, along with Eq. (22), can then be used to implement this method in ANSYS.

The solution technique used was to solve Eqs. (15) through (20), by the implicit finite difference method on a deforming grid. The equations were rewritten according to a central difference scheme, using the Crank-Nicholson method [cf. 7]. Temperature dependent material properties were handled by computing properties at each node at the beginning of each time step, and holding the value constant over that time step.

The procedure for evaluating the boundary conditions at the wet sand/dry sand interface was as follows:

(i) From the present values of the temperature distribution, calculate the interface speed using Eq. (17).

(ii) Step the vapor line to the position it will occupy at time $t + \Delta t$.

(iii) Regenerate the finite difference grid to be uniform over the new domain, keeping the same number of grid points.

(iv) Interpolate the temperature distribution onto the new grid locations at the present time step.

(v) Fix the temperature at $r = R_o + n\delta$ to T_s (Eq. (20)).

(vi) Calculate the new temperature distribution at time $t + \Delta t$ using the implicit finite difference scheme.

(vii) Return to step (i), and continue until the desired stopping time is reached.

This scheme, like most schemes of this type, is not self-starting, i.e., if the initial conditions given in Eqs. (19) and (20) were to be used, the vapor line would not be explicitly generated. To get around this problem, the solution was started by using the known, exact solution for heat flow from a plane surface with the boundary condition $T = T_w$ at R_o, given in Eqs. (11) through (13). This solution was applied at $t = 1$ second, and then the finite difference scheme took over to generate the rest of the solution. Shorter values for the starting time were used when the radius of curvature was very small, so that in no case did the starting value for δ exceed $R_o/10$.

The starting solution must be adjusted, slightly, because the actual temperature in the mold at the wall at time $t = 1$ second is not equal to T_w, due to the finite resistance to heat flow at the interface. To obtain a good starting solution, the heat fluxes at the wall in the two solutions were matched. In equation form, this means that the starting wall temperature, T_1^1, must be chosen such that

$$-\kappa \frac{\partial T_{start}}{\partial x} \Big|_{x = 0} = h(T_1^1 - T_w) \qquad (23)$$

Here, $\partial T_{start}/\partial x$ is evaluated using the exact solution, Eq. (14).

The finite difference technique was first validated by letting $h \to \infty$ on a plane surface ($a = 0$), using constant material properties, and comparing the computed results to the exact solution given in Eqs. (11) through (13). With 21 grid points, and time steps equal to $0.9\{\kappa/\rho C_p(\Delta r)^2\}$ (twice the value available in explicit methods), the computed temperatures and positions of the vapor line were always within 3 percent of the exact solution.

A series of calculations was then performed for the geometries of interest. The sand mold was assumed to be of constant density, 1.565 g/cm^3, to contain 4 percent water, and the specific heat and thermal conductivity were as shown in Figs. 5 and 6. The heat transfer coefficient was taken to be constant, 0.0015 W/(mm^2 K).

Some representative results of the calculations are given in Fig. 7. Shown are computed temperature distributions in the sand at various times outside a plane wall held at 1000 C. Similar results occur for heat flow outside cylinders and spheres. An interesting special case appears when considering convergent heat flow in a cylinder or sphere. At some time, the vapor line reaches the origin, corresponding to the complete removal of binder from the mold. When this occurs, the heat transfer mechanism is simply heating of the enclosed region, without any vaporization. The boundary condition at $r = 0$ must then changed to be

$$\frac{\partial T}{\partial r} = 0 \text{ at } r = 0 \qquad (24)$$

Results for a representative case are presented in Fig. 8. These cases are important, because they represent heat flow in cores internal cavities, or near re-entrant corners. The point where the vapor line reaches the center corresponds to saturation of the core or cavity.

(c) Implementation in ANSYS

It was immediately apparent that none of the standard ANSYS elements would suit for the implementation of the methods described above. Swanson Analysis provided the source code for one of their standard elements, STIF6, to allow modification of the element to accept the boundary conditions derived from the above solutions.

In STIF6, the expected form for the heat flux from the surface defined by the STIF6 element is [8]

$$q = h_{eff} (T - T_o) \tag{25}$$

and

$$h_{eff} = \left(\frac{1}{HF(T - T_o)^n} + \frac{1}{C}\right)^{-1} \tag{26}$$

where HF is interpreted as a heat transfer coefficient and may depend on temperature, C may be a function of the total heat which has flowed through the surface, per unit area and T_o is a reference temperature.

It is easiest to see how to recast the above solutions in a form close to this one by returning to the analytical solution for the plane with fixed temperature, Eq. (14). The heat flux was given by

$$q(t) = \frac{T_w - T_s}{\text{erf } \gamma} \cdot \frac{\kappa}{\sqrt{\pi \alpha t}} \tag{27}$$

The total heat to flow through the surface, per unit area, is then

$$\text{QTOTAL} = \int_0^t q(t)\, dt = \frac{T_w - T_s}{\text{erf } \gamma} \cdot \frac{2\kappa}{\sqrt{\pi \alpha}} t^{1/2} \tag{28}$$

To adopt a form like Eq. (25) for q, one may ignore HF, set $T_o = T_s$, and obtain

$$q = C(\text{QTOTAL})(T_w - T_s) \tag{29}$$

Equating q in Eqs. (27) and (29) yields C as a function of time

$$C(t) = \frac{\kappa}{\text{erf } \gamma \sqrt{\pi \alpha}} t^{-1/2} \tag{30}$$

and then comparing Eqs. (28) and (30) to eliminate t yields

$$C(\text{QTOTAL}) = \frac{1}{\text{QTOTAL}} \cdot \left\{\frac{\kappa}{\text{erf } \gamma \sqrt{\pi \alpha}}\right\}^2 \{2(T_w - T_s)\} \tag{31}$$

An important feature of Eq. (31) is that C is not only inversely proportional to QTOTAL, but it is also proportional to $(T_w - T_s)$. Thus, in the case where the surface temperature changes over the time of the simulation, this factor must change as well. It is this result which necessitated the modification of STIF6. In accord with the assumption that the surface temperature changes slowly compared with heat flow in the sand, the implementation of Eq. (31) is as follows:

(i) Compute and store C(QTOTAL) for a single wall temperature called T_{wo}.

(ii) After using the table to obtain C(QTOTAL), adjust the value by multiplying by a factor based on the actual wall temperature, T:

$$C_{actual} = C(QTOTAL) \times \frac{T - T_s}{T_{wo} - T_s} \qquad (32)$$

In view of Eq. (22), the correction can be applied at each time step. This procedure was put into STIF6, and was used in the example calculations given in the next section.

For the case having temperature dependent properties and a convective heat transfer coefficient boundary condition at the sand-metal interface, the relationship implied by Eq. (32) was evaluated. Figure 9 shows a plot of C(QTOTAL), normalized as in Eq. (32), vs. QTOTAL, for simulations run using various values of T_w on a plane wall. For practical purposes, the data lie on a single curve. The curve is nearly a straight line in a log-log plot, with slope close to -1, as one would get from Eq. (31). This indicates that the actual heat flow problem is quite similar to the ideal case. This point has been made only to elucidate the physics of the problem; in the examples which follow, the numerical results were used.

The catalog of solutions to the heat flow problems described in the previous section may now be written in terms of the C and QTOTAL functions. C and QTOTAL were determined for various values of radius for spheres and cylinders, as well as for the plane. The reference wall temperature used was 1000 C. The results are shown in Figs. 10 through 13.

The heat flow outside of a curved surface can be seen to decrease as the radius increases. Once the radius exceeds about 200 mm for either the cylinder or the sphere, the C versus QTOTAL curve is equivalent to the curve computed for the plane. This indicates that the practical limit for curvature of the surface to affect the heat flow is about 200 mm. For inward directed

heat flow, the saturation point can be seen to increase continuously with radius.

EXAMPLE

The method described in the last sections was used to simulate the solidification of a 169 mm diameter cast iron sphere in a water bonded sand mold. This problem was chosen because it is one for which experimental data exist [9], and also because it had been successfully simulated before, including nodes in the sand mold [4]. Furthermore, since the curvature of the sphere is known and constant over the entire simulation, the results were expected to be very good for this case.

The thermal properties for the iron used in the simulation were as shown in Figs. 14 through 16. Some results of the simulation are given in Figs. 17 and 18, in which computed temperatures are compared with experimentally determined values for two locations in the sphere. The agreement between the calculated values and the experimental results is quite satisfactory. This simulation consumed approximately 1200 cpu seconds on a PRIME 750. This is about 65 percent of the cpu time required for the identical problem with the sand mold in place [4]. The results from the two simulations were equivalent.

DISCUSSION

Several phenomena which are known to occur in foundry casting have been neglected in the analysis. Among these are the formation of a steam layer between the casting and the mold for short times after pouring; recondensation of binder in the wet wand at some distance from the vapor line; and conduction of heat in the wet sand. The overall impact of each of these effects on the solution should be relatively small in comparison to the heat flow effects which have been modeled. It is intended to include some of these refinements in future work.

The utility of this method will rely upon automating the selection of curvatures and surfaces. This task is underway, and will be described in a subsequent paper. Another pending task is the determination of the number of changes in curvature over the course of a simulation which is necessary to obtain satisfactory results. Finally, several complex castings need to be simulated, and the results compared to experiments to prove the method.

CONCLUSIONS

1. A method for replacing the modeling of heat flow in bonded sand molds, by boundary conditions on the casting alone, has been developed. The method consists of representing the local surface geometry by a plane, sphere, or cylinder, based on the local heat flow environment. The characteristics of the heat flow into the mold for that surface shape are then used to specify the boundary conditions on the casting.
2. A method for solving the heat flow problem in various sand molds has been presented, along with several example solutions.
3. These solutions have been used to construct boundary conditions, and implementation in a FEM program has been accomplished.
4. Simulation of a 169 mm cast iron sphere has been run, using the new method. The results agree well with experimental data, and have reduced cpu time to about 65 percent of the time required equivalent simulations with sand present, with equivalent results.
5. Remaining tasks include:
   a. Automation of generation of surface element characteristics;
   b. Obtaining accurate benchmarks to document savings;
   c. Consideration of more complicated castings, and comparison with experiments.

ACKNOWLEDGMENT

This work has been supported by the Materials Processing Consortium at the University of Illinois, sponsored by Deere and Company, Caterpillar Tractor, General Motors, and TRW. The calculations were performed on a PRIME 750, located at Deere and Company Technical Center. B. Romig, M. Robinson, and N. Lillybeck of Deere and Company contributed significantly to the course of the work. Dr. J. Swanson, of Swanson Analysis Systems, in providing the source code for STIF6, was indispensable.

REFERENCES

1. E. Niyama, J. Japan Foundrymen's Society, 1977, Vol. 49, p. 26.

2. C. Wei, P. N, Hansen, and J. T. Berry, Numerical Methods in Thermal Problems, 1981, Vol. 2, pp. 193-204, Pineridge Press, Swansea,.

3. C. Wei, J. T. Berry, and P. H. Franklin, in press, Modeling of Casting and Welding Processes, Vol. 2, J. A. Dantzig and J. T. Berry, Eds., TMS-AIME, Warrendale, 1984.

4. M. Robinson, Deere and Company Technical Center, Moline, IL, private communication, 1983.

5. M. C. Flemings, Solidification Processing, p. 17, McGraw-Hill, New York, (1974).

6. H. S. Carslaw and J. C. Jaeger, Conduction of Heat in Solids, 2nd Edition, p. 31, Oxford University Press, London, (1965).

7. C. F. Gerald, Applied Numerical Analysis, 2nd Edition, pp. 392-410, Addison-Wesley, Reading, MA, 1978.

8. G. S. DeSalvo and J. A. Swanson, ANSYS Theoretical Manual, Section 4.6, Swanson Analysis Systems, Inc., Houston, PA, 1983.

9. C. A. Sanders and R. L. Doelman, AFS Transactions, 1971, Vol. 79, p. 1, 1971.

LIST OF FIGURES

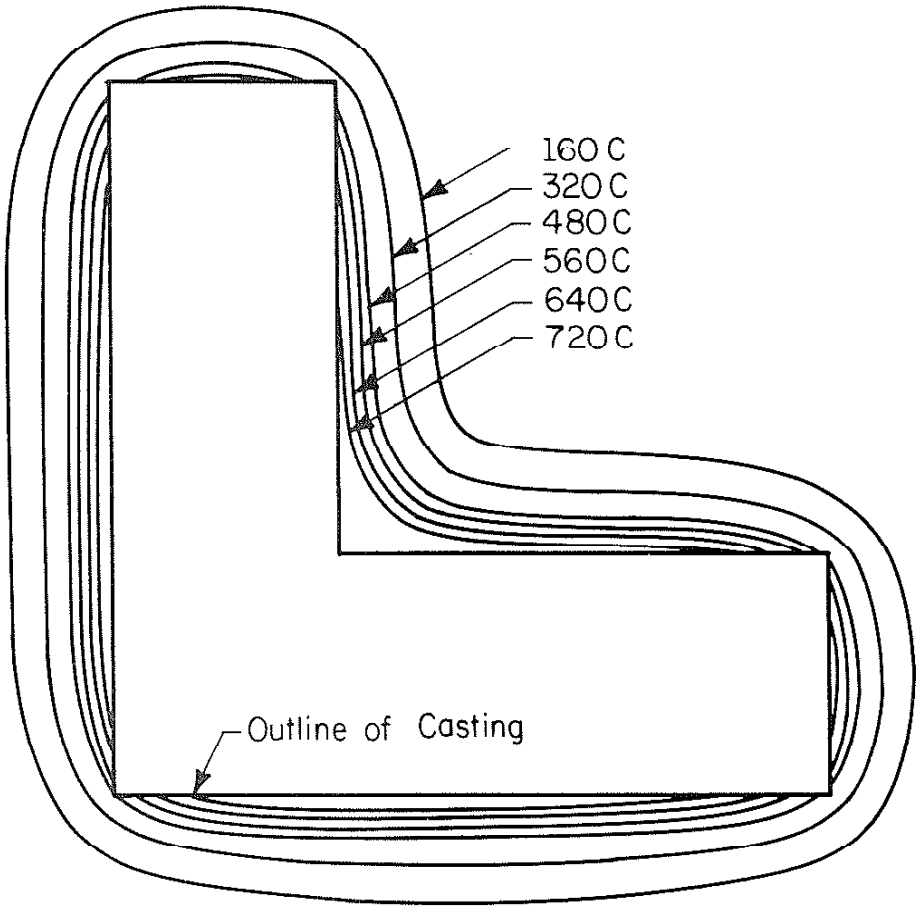

Figure 1 Computed Isotherms in Sand Mold Outside a Two-Dimensional L-Shaped Plate 549 Seconds after Pouring (Courtesy M. Robinson [4]).

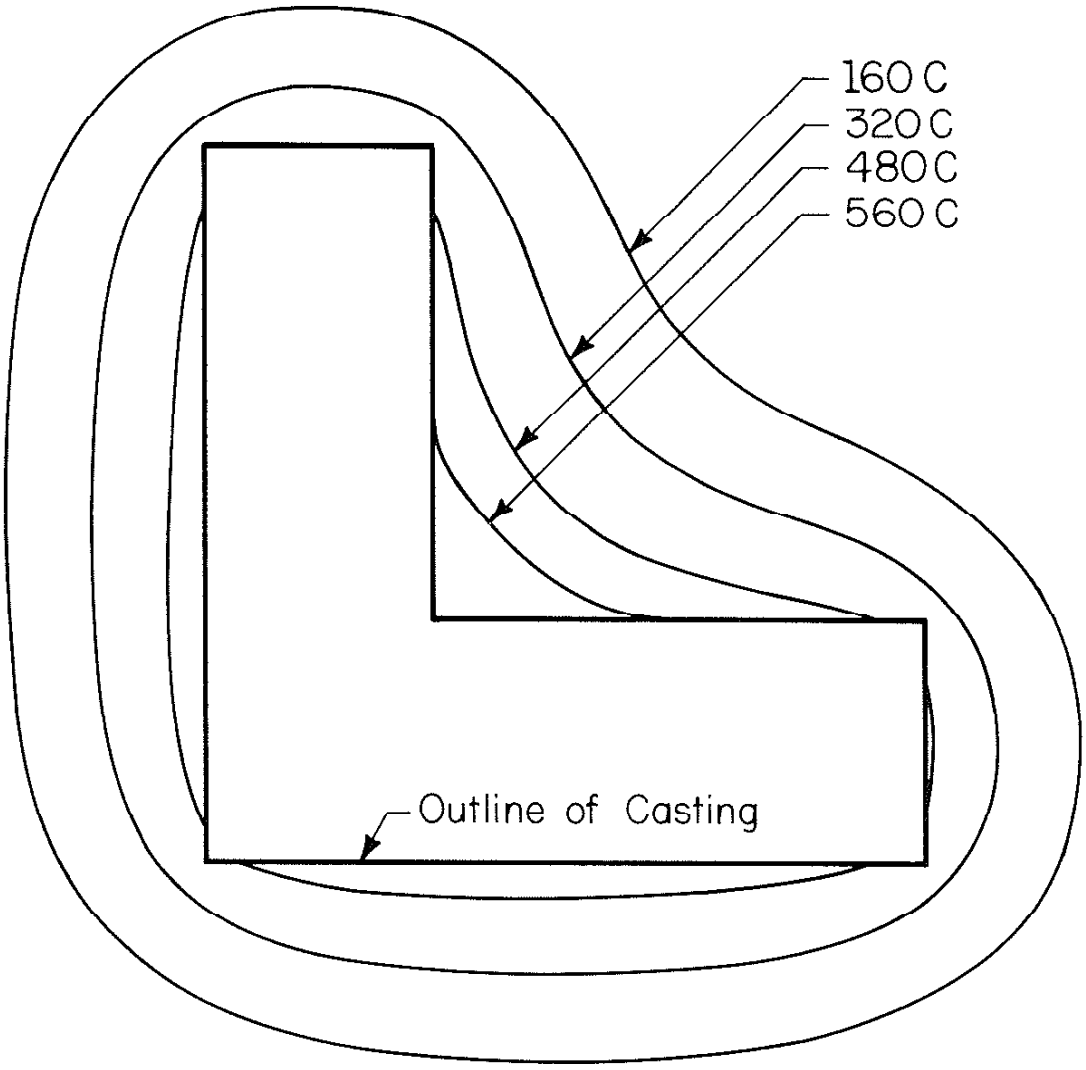

Figure 2 Computed Isotherms in Sand Mold Outside a Two-Dimensional L-Shaped Plate 2950 Seconds after Pouring (Courtesy M. Robinson [4]).

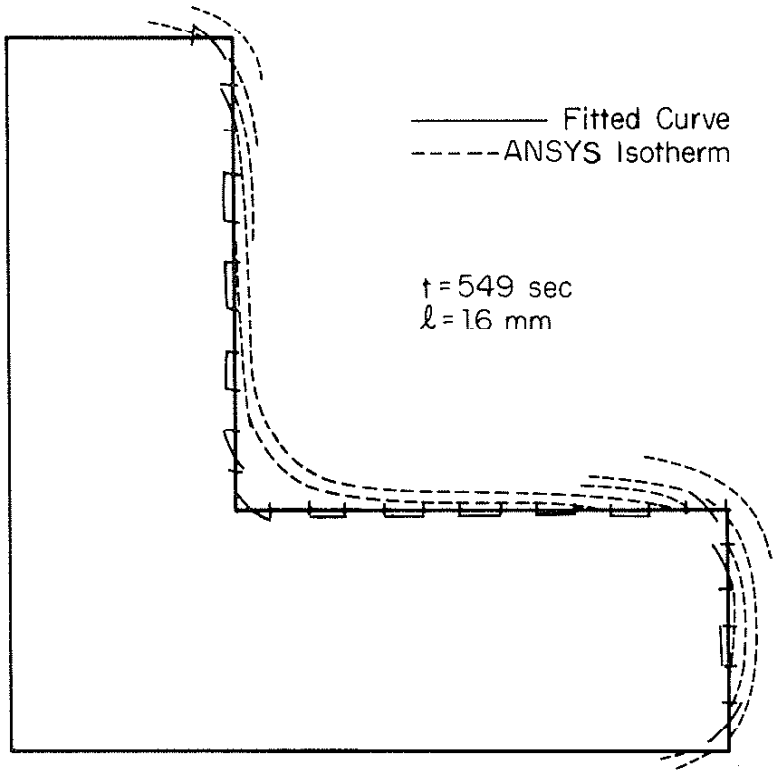

Figure 3 Comparison of Fitted Surface Shape and Computed Isotherms in Sand 549 Seconds after Pouring.

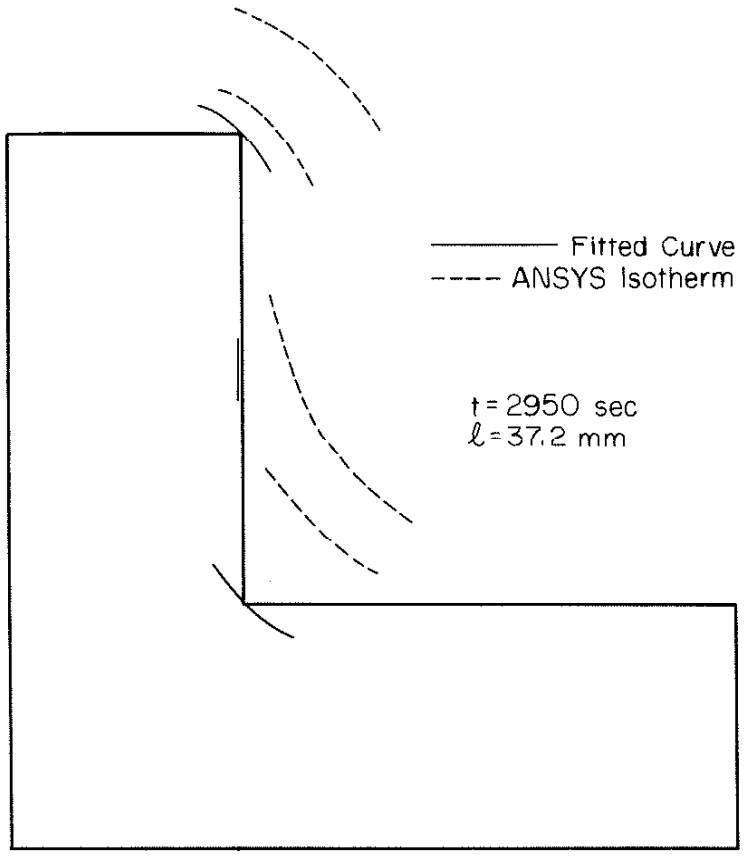

Figure 4 Comparison of Fitted Surface Shape and Computed Isotherms in Sand 2950 Seconds after Pouring.

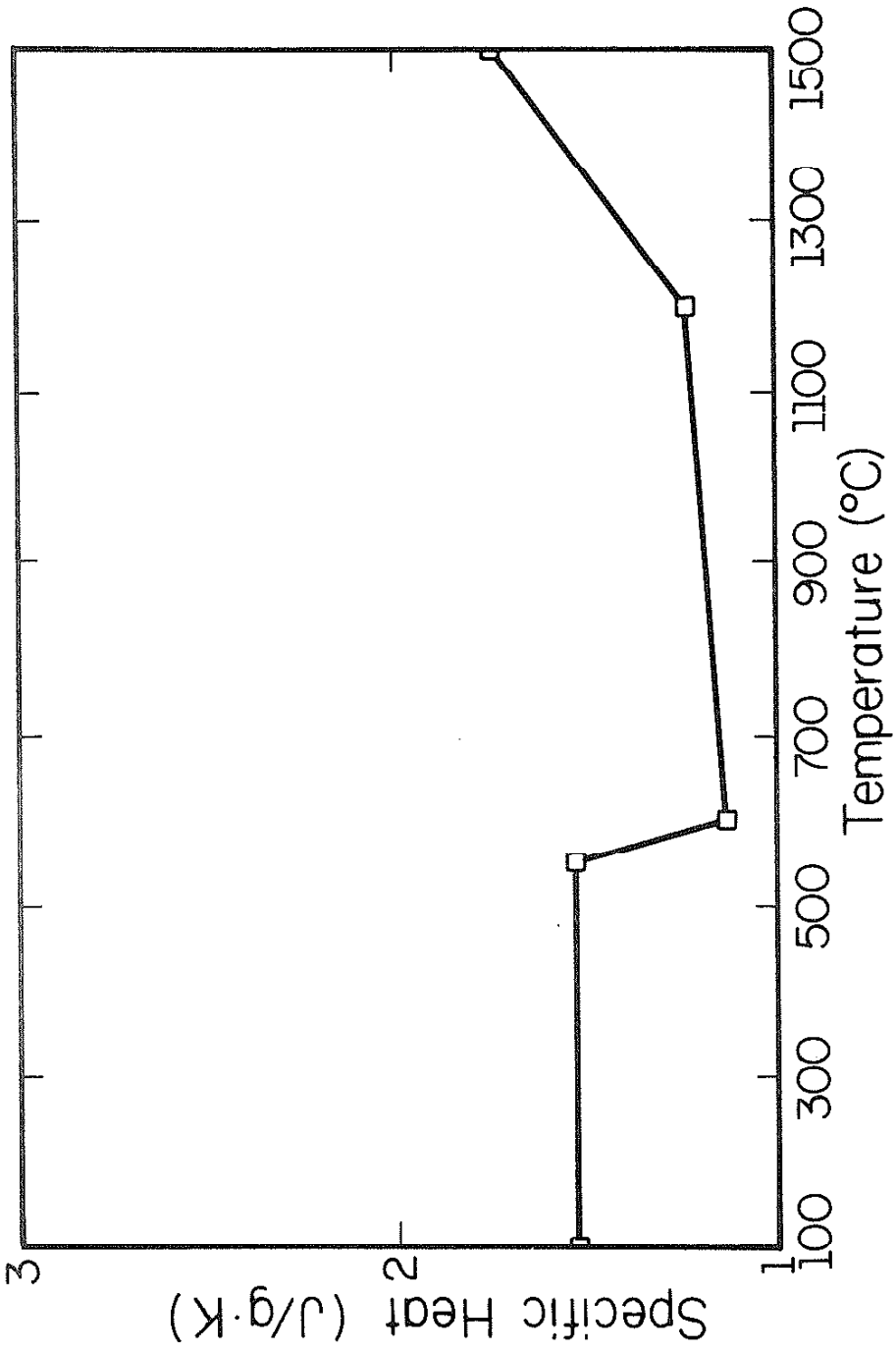

Figure 5 Specific Heat of Dry Sand versus Temperature Used in Calculations.

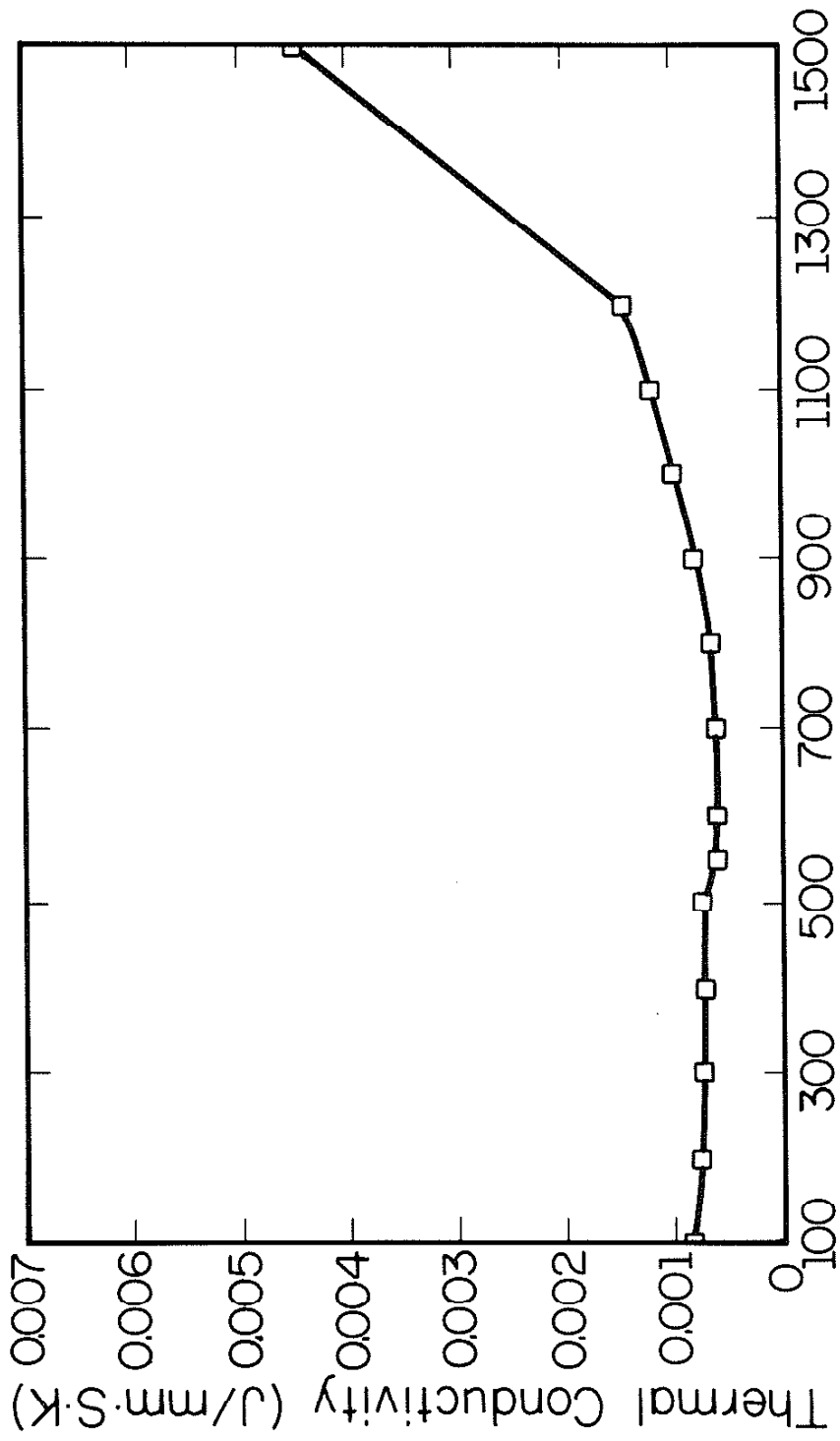

Figure 6 Thermal Conductivity of Dry Sand versus Temperature Used in Calculations.

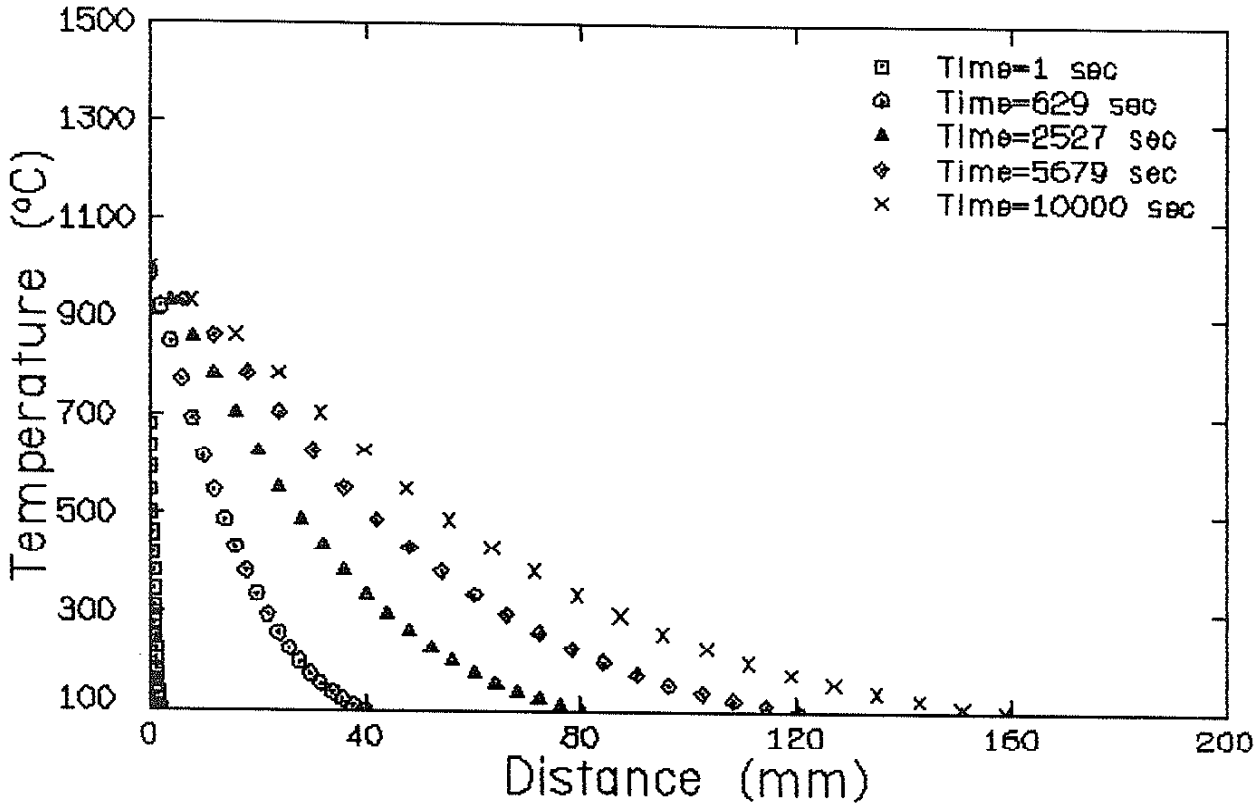

Figure 7 Calculated Temperature Distribution in the Mold Outside a Plane Surface at Various Times.

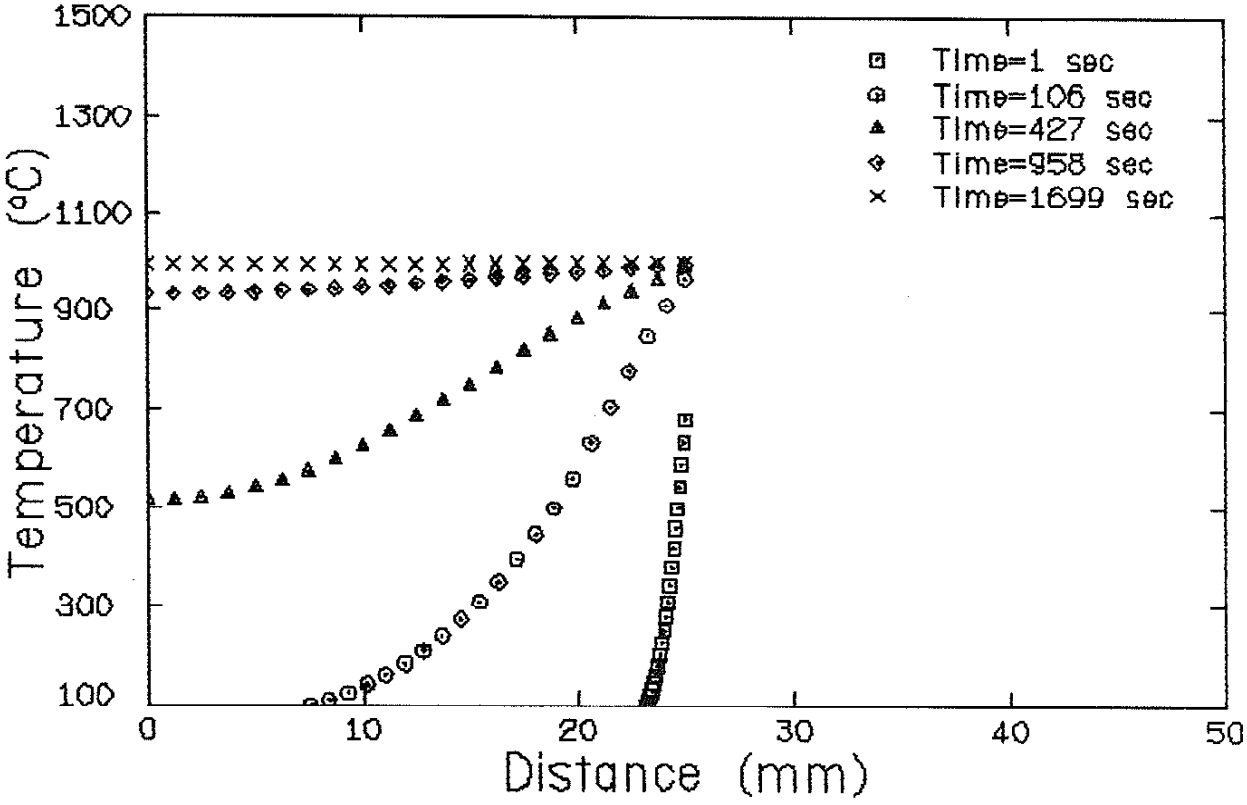

Figure 8 Calculated Temperature Distribution in the Mold Inside a 50 mm Diameter Cylinder.

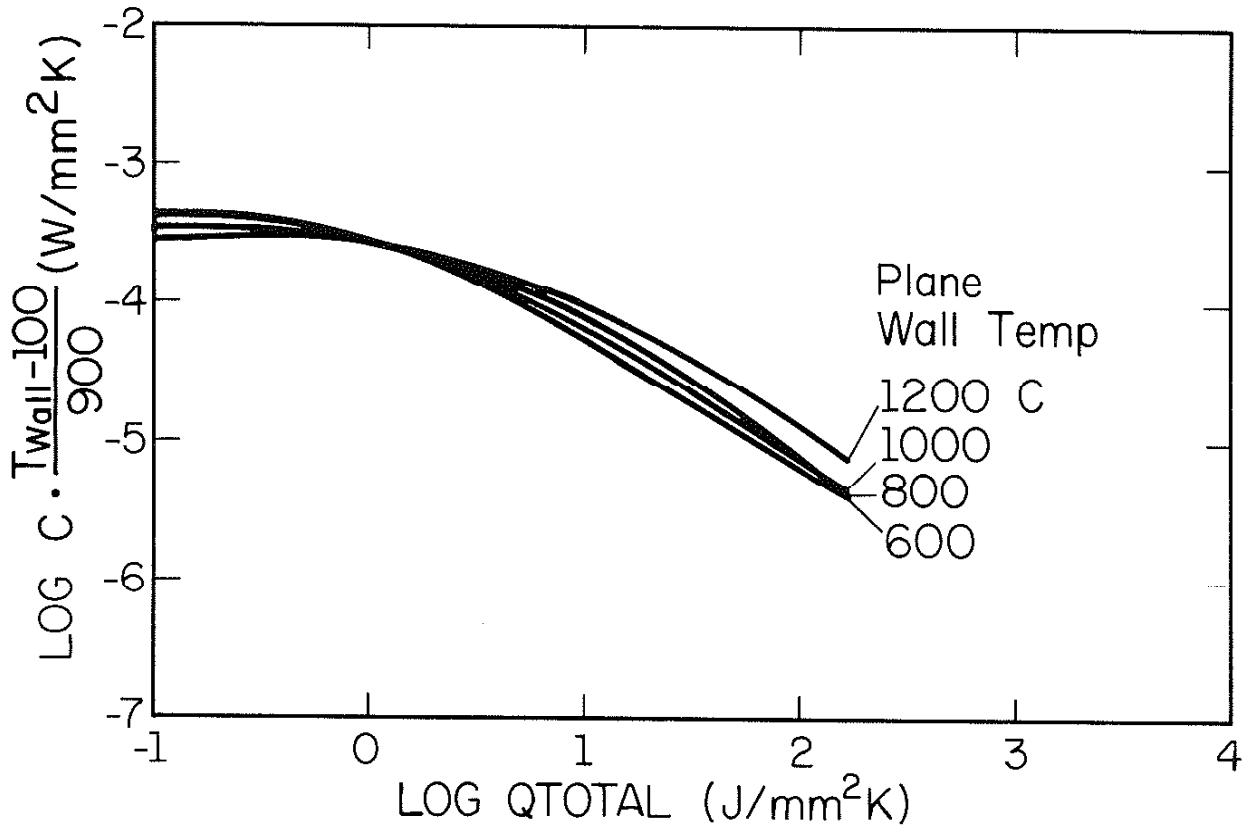

Figure 9 Normalized Effective Heat Transfer Coefficients (C) versus Accumulated Heat Flux (QTOTAL) through a Plane Wall at Several Temperature.

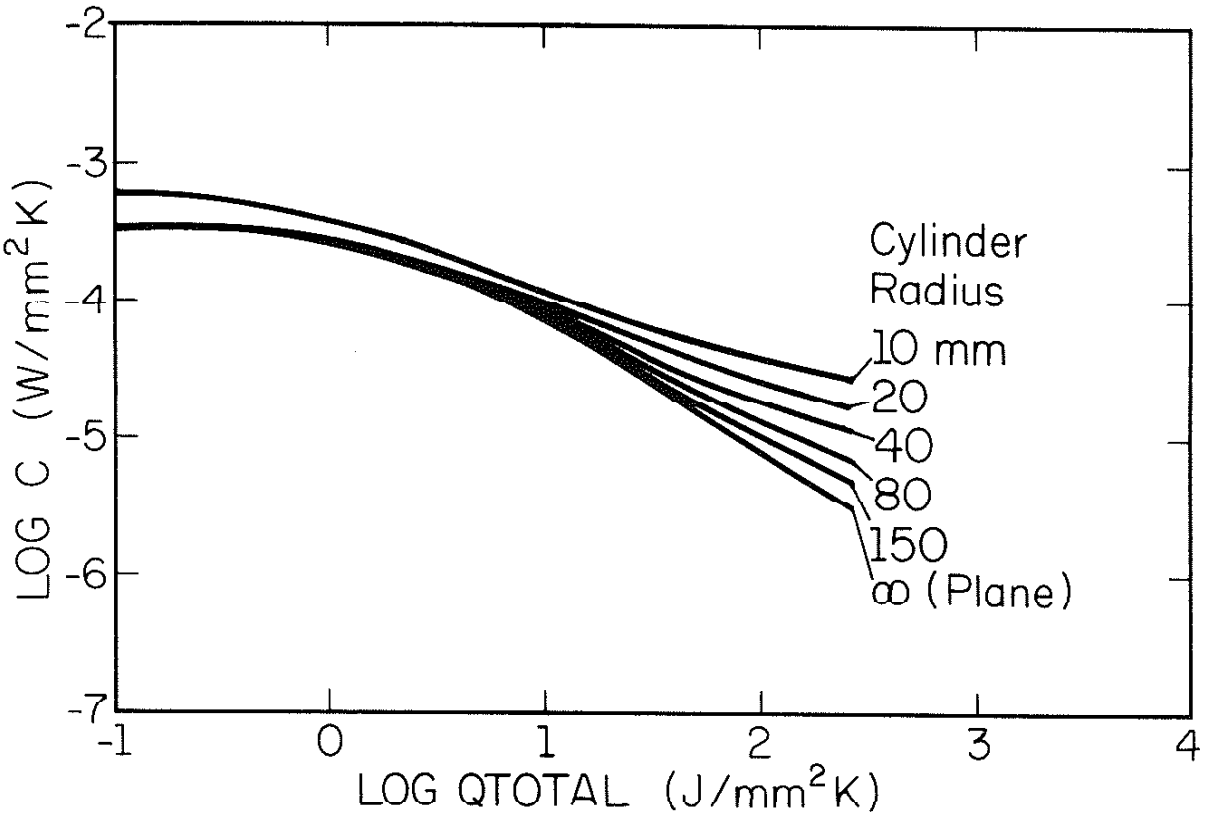

Figure 10 Computed Effective Heat Transfer Coefficients versus Accumulated Heat Flux through Divergent Cylindrical Walls of Various Radii, at 1000 C.

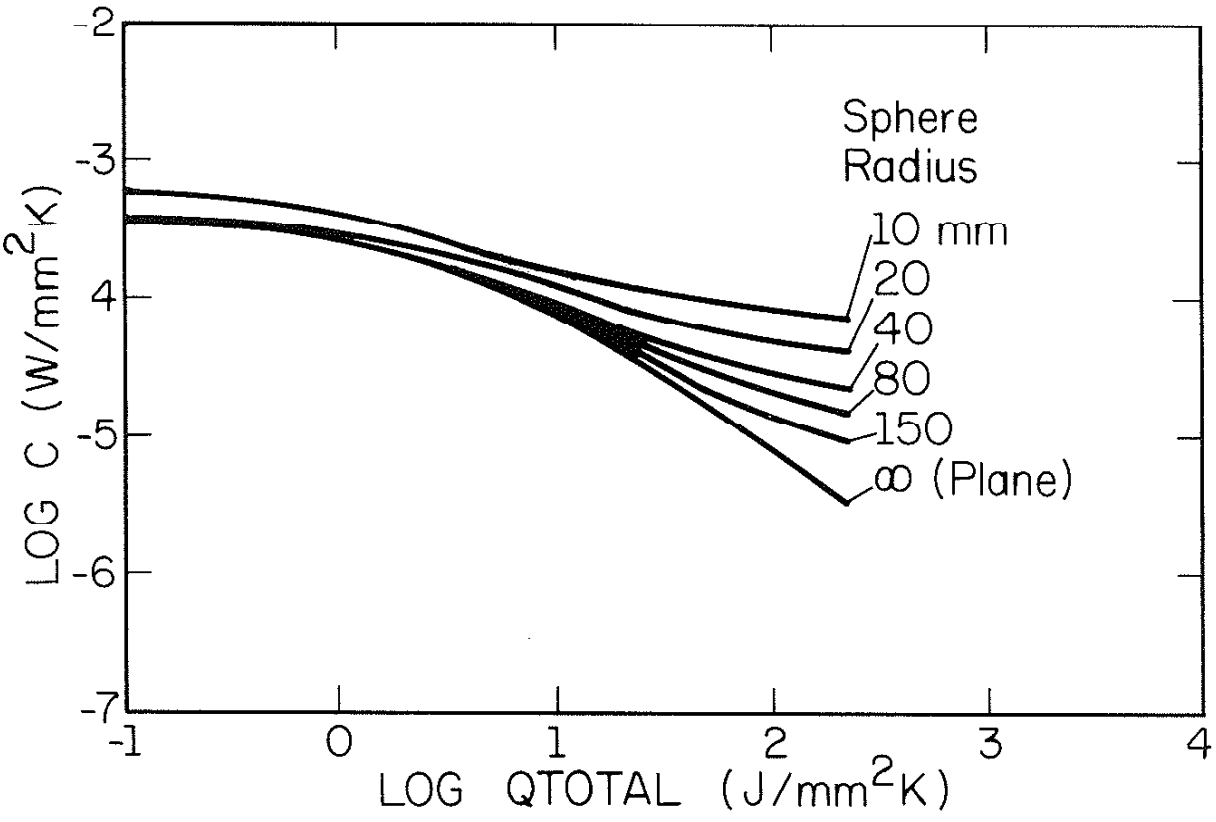

Figure 11 Computed Effective Heat Transfer Coefficients versus Accumulated Heat Flux through Divergent Spherical Walls of Various Radii, at 1000 C.

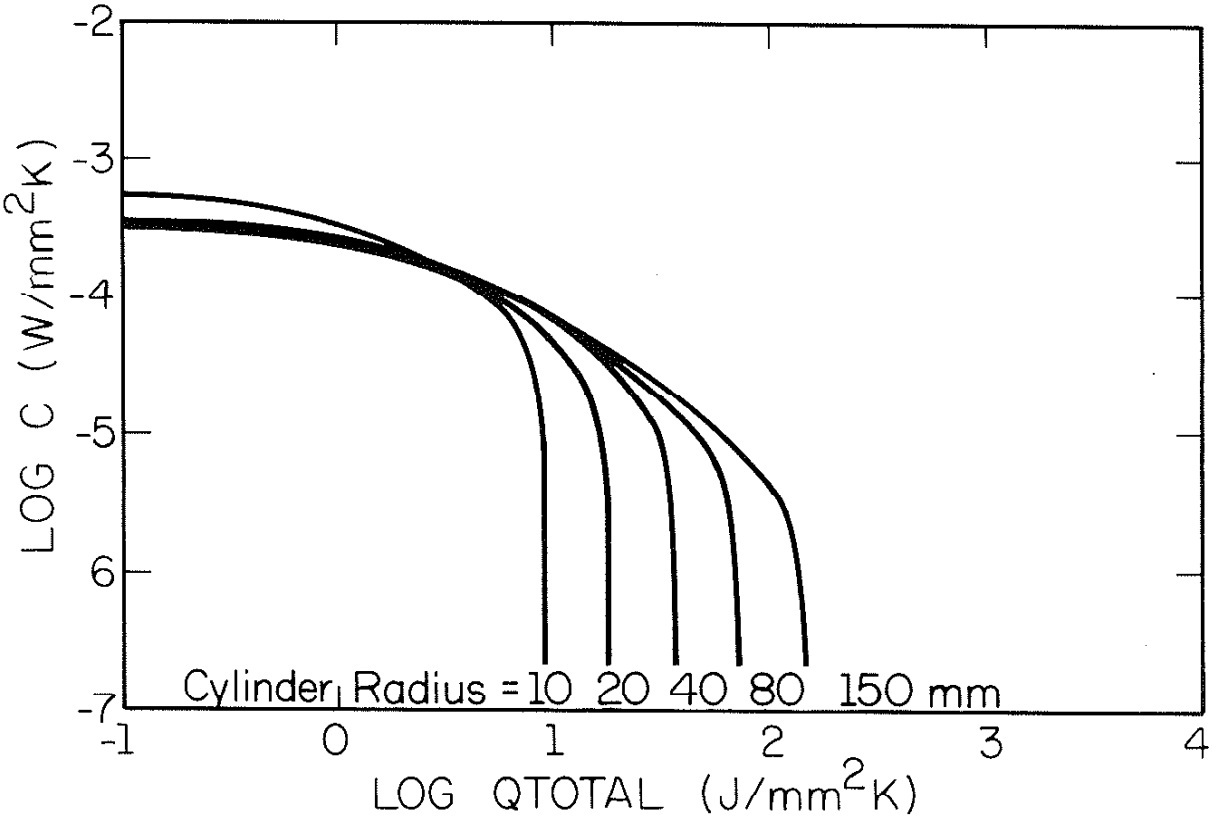

Figure 12 Computed Effective Heat Transfer Coefficients versus Accumulated Heat Flux through Convergent Cylindrical Walls of Various Radii, at 1000 C.

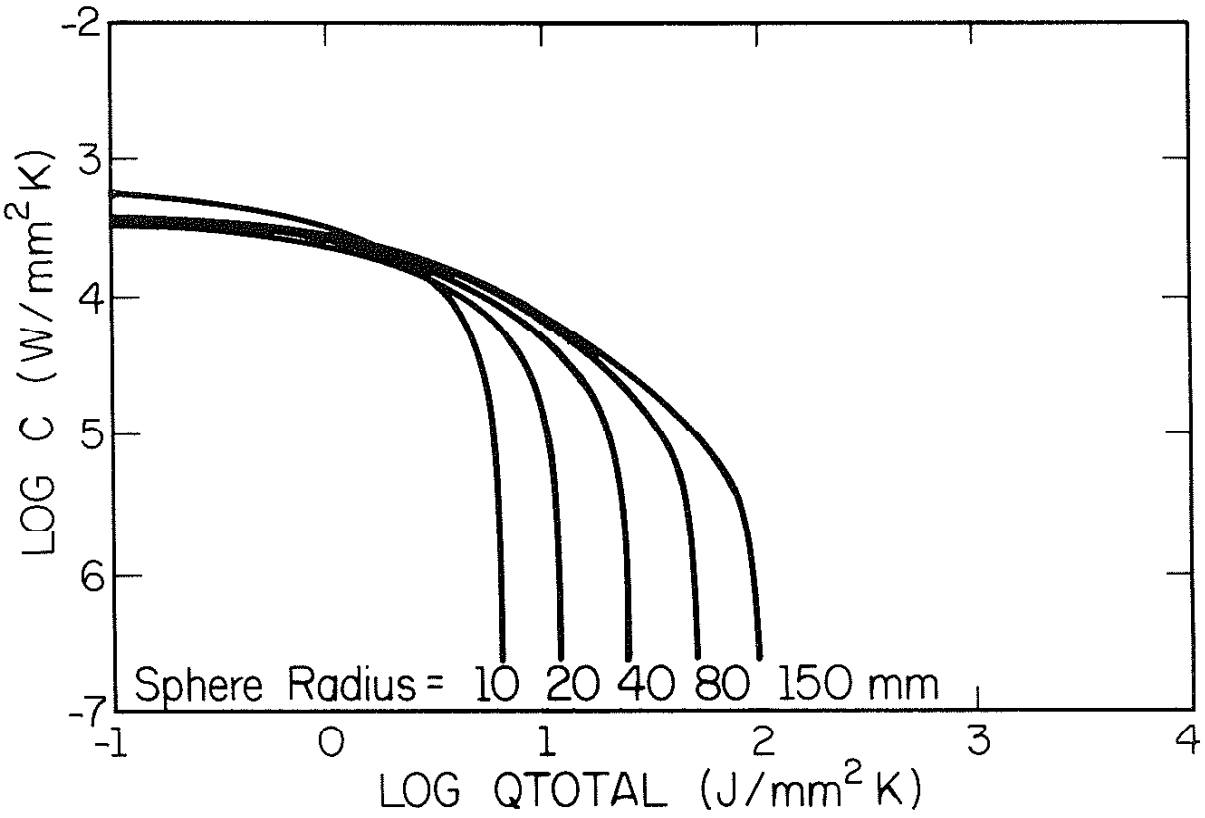

Figure 13 Computed Effective Heat Transfer Coefficients versus Accumulated Heat Flux through Convergent Spherical Walls of Various Radii, at 1000 C.

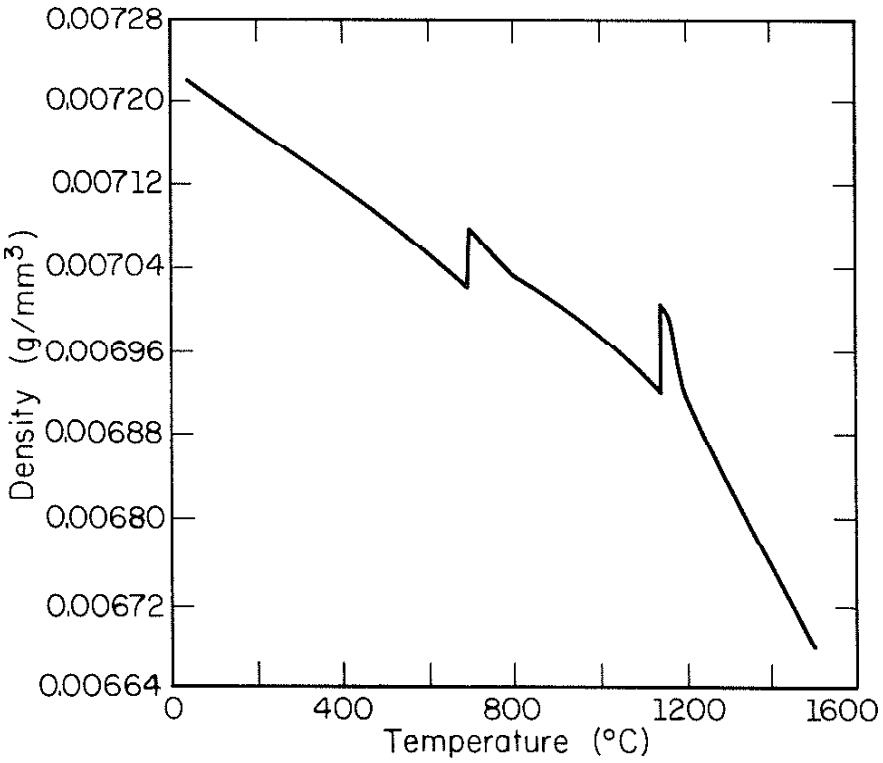

Figure 14 Density of Iron versus Temperature Used in Simulations.

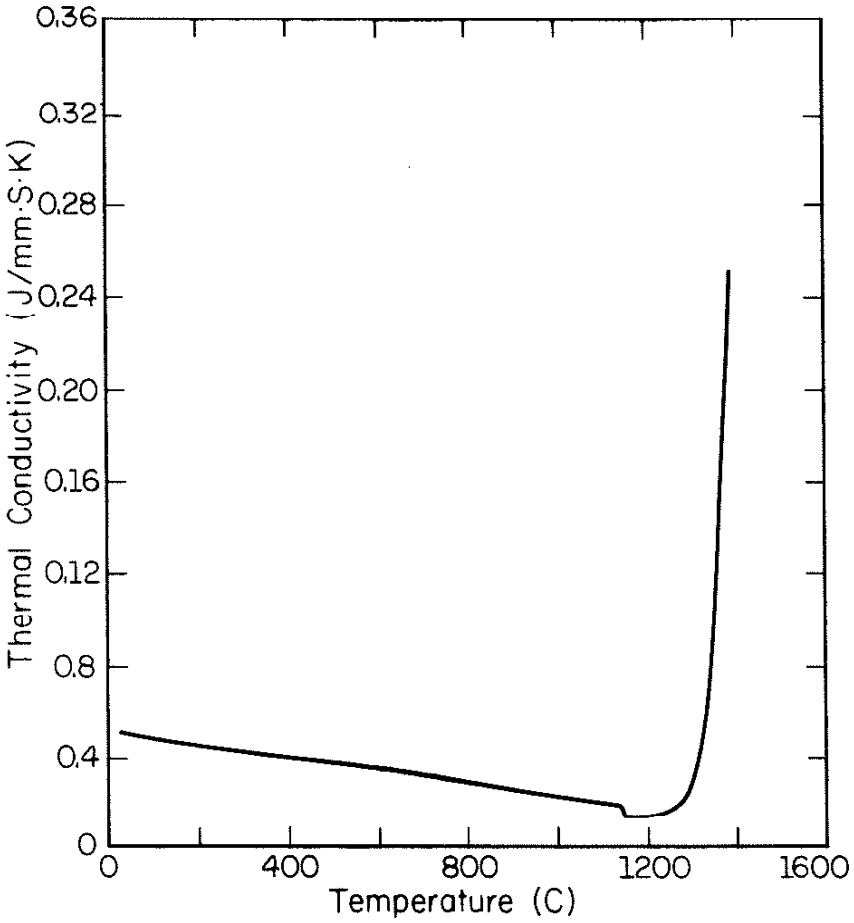

Figure 15 Thermal Conductivity of Iron versus Temperature Used in Simulation. Liquid Conductivity was Artificially Increased to Represent Convection.

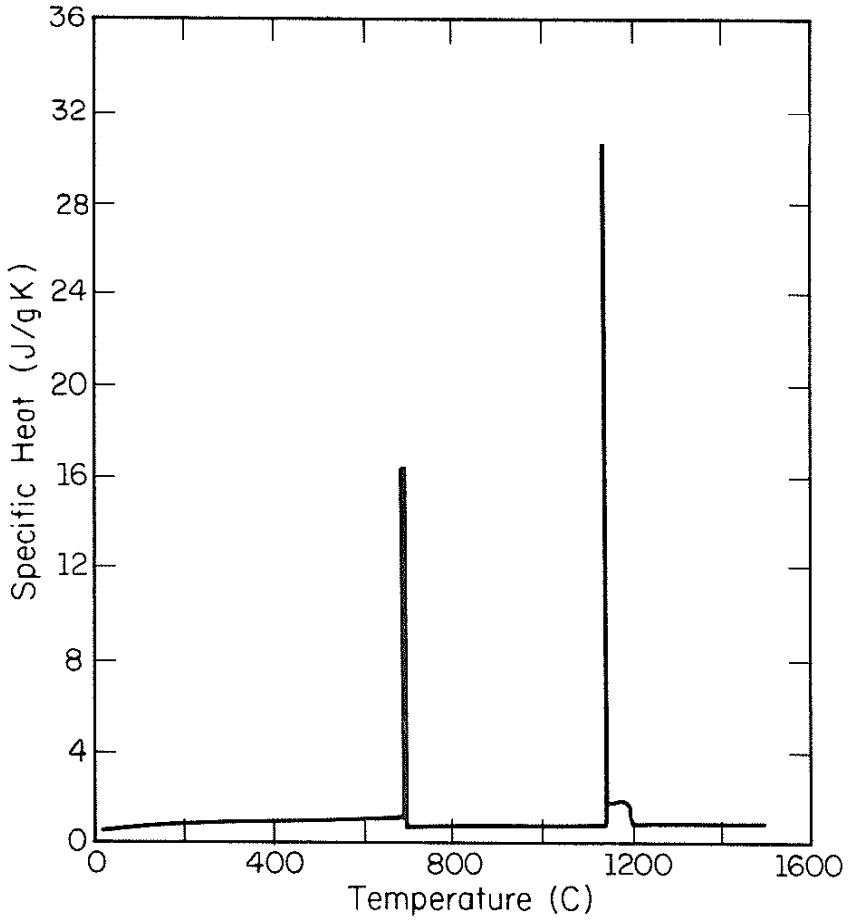

Figure 16 Specific Heat of Iron versus Temperature Used in Simulations.

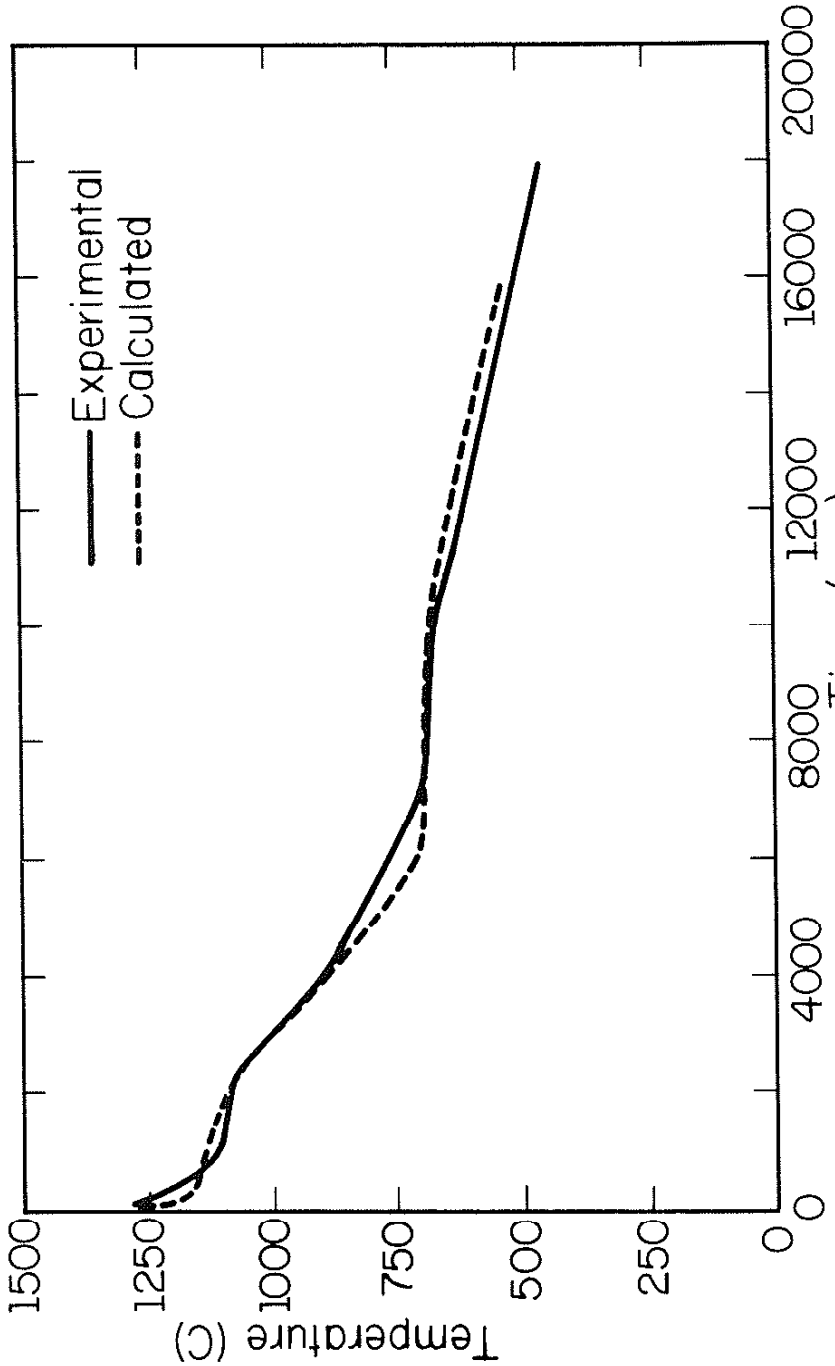

Figure 17 Comparison of Computed and Experimental Cooling Curves
6.35 mm Inside a 169 mm Diameter Cast Iron Sphere.

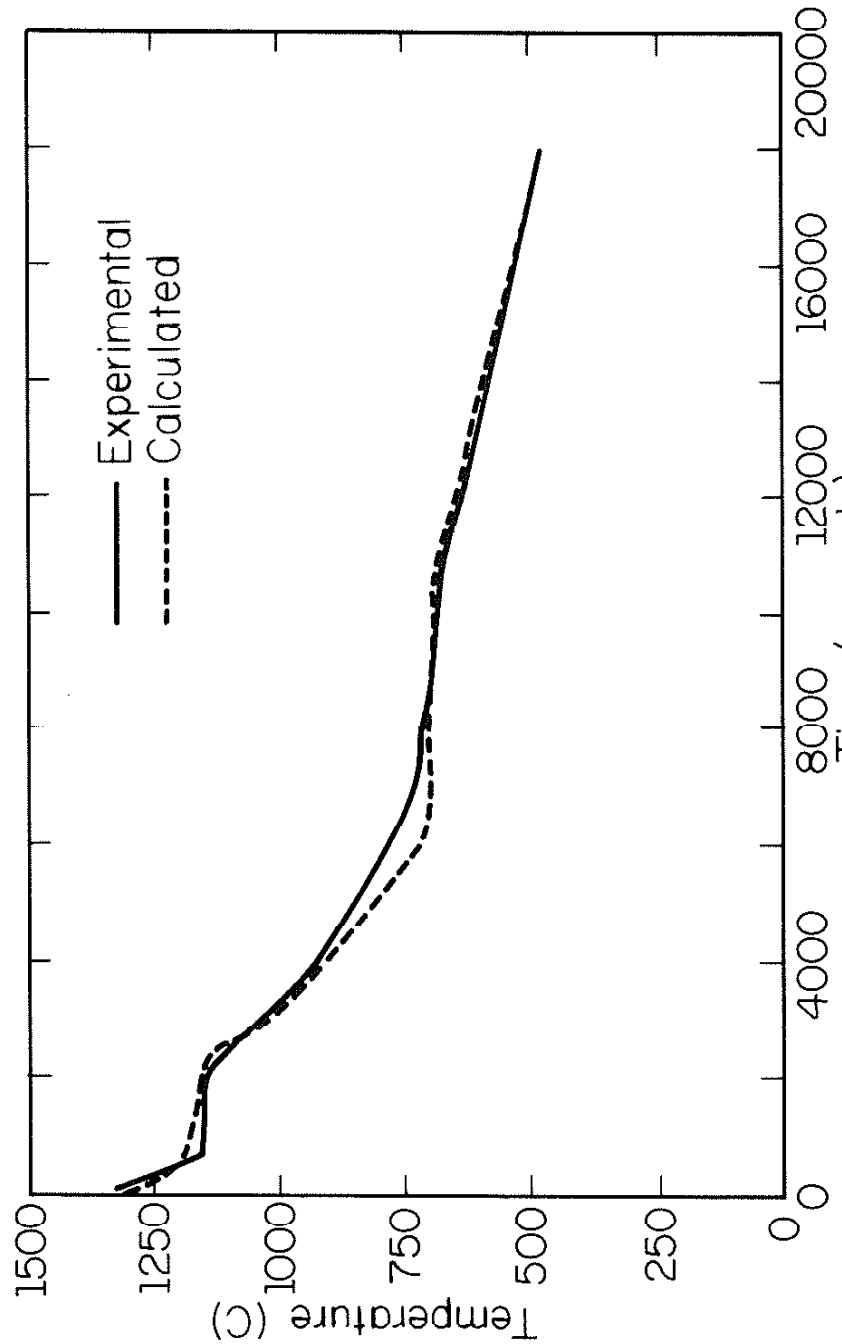

Figure 18 Comparison of Computed and Experimental Cooling Curves
50.8 mm Inside a 169 mm Diameter Cast Iron Sphere.